DEPARTMENT OF THE AIR FORCE
AIR FORCE RESEARCH LABORATORY
WRIGHT-PATTERSON AIR FORCE BASE OHIO 45433

8 May 2001

MEMORANDUM FOR US EPA
NCEA (MD-52)
RTP, NC 27711
ATTN: ANNIE M. JARABEK

FROM: Elaine Merrill
AFRL/HEST
Operational Toxicology Branch
2856 G St, Bldg 79
Wright-Patterson AFB, OH 45433-7400

SUBJECT: Consultative Letter, AFRL-HE-WP-CL-2001-0005, PBPK Model for Iodide Kinetics and Perchlorate-Induced Inhibition in the Male Rat.

1. This letter describes a physiologically-based pharmacokinetic (PBPK) model for predicting the inhibition of thyroid iodide uptake after exposure to perchlorate (ClO_4^-) in the male rat. The model is a continuation of the preliminary work presented in Consultative Letter, AFRL-HE-WP-CL-2000-0035, Physiological Model for Inhibition of Thyroidal Uptake of Iodide by Perchlorate in the Rat. The new model structure improves prediction of inhibition of iodide uptake by perchlorate at doses ranging over three orders of magnitude. This refined model also incorporates compartments that will be necessary in the development of a pharmacodynamic model to predict thyroid hormone perturbations.

2. For further information, please contact me by phone: (937) 255-5150 ext. 3195, fax: (937) 255-1474 or e-mail: elaine.merrill@wpafb.af.mil.

Elaine A. Merrill

ELAINE A. MERRILL
Operational Toxicology Branch

Attachment:
PBPK Model for Iodide Kinetics and Perchlorate-Induced Inhibition in the Male Rat

1st Ind, AFRL/HEST 8 May 2001

MEMORANDUM FOR US EPA
ATTN: MS. ANNIE JARABEK

This letter report has been coordinated at the branch level and is approved for release.

RICHARD R. STOTTS, DVM, PhD
Branch Chief
Operational Toxicology Branch
Human Effectiveness Directorate

PBPK Model for Iodide Kinetics and Perchlorate-Induced Inhibition in the Male Rat

Elaine A. Merrill[1], Rebecca A. Clewell[2], Jeffery M. Gearhart[3], Peter J. Robinson[3], Teresa R. Sterner[1], Latha Narayanan[2], Kyung O. Yu[4] and Jeffrey W. Fisher[4*]

[1]Operational Technologies, Corp.
1370 N. Fairfield Rd., Ste. A
Dayton, OH 45432

[2]GEOCENTERS, Inc.
2856 G St, Bldg 79
Wright-Patterson AFB, OH 45433

[3]ManTech Environmental Technology, Inc.
2856 G St, Bldg 79
Wright-Patterson AFB, OH 45433

[4]AFRL/HEST
2856 G St, Bldg 79
Wright-Patterson AFB, OH 45433

[*]Current Address:
Department of Environmental Health Science
The University of Georgia
206 Environmental Health Science Bldg
Athens, GA

8 May 2001

INTRODUCTION

Perchlorate is a monovalent anion similar in charge, shape and size to iodide. It is not metabolized and is rapidly excreted in urine; however, while in the body perchlorate competitively inhibits iodide uptake in the thyroid and other tissues. For that reason, perchlorate has been used therapeutically to treat hyperthyroidism (Wolff, 1998). If administered within hours of an accidental or excessive exposure to radioiodide, it can serve as a safe and effective prophylaxis (thyroid uptake blocking agent) (Ribela *et al.*, 1999). Commercially, the salt (ammonium perchlorate) is used for its strong oxidizing properties in rocket fuel and fireworks. Perchlorate contamination has been recently detected in several water sources (Urbansky and Schock, 1999). As a result, there is concern that chronic exposure to low levels in drinking water could lead to hypothyroidism and possibly mental retardation in newborns exposed during gestation or nursing (Bernal and Nunez, 1995; Hetzel, 1983).

Limited studies have been conducted on the kinetics of perchlorate in animals. Higher than serum concentrations of iodide and perchlorate have been noted in the thyroid, adrenal glands, bile, spleen, gastric mucosa, salivary glands, mammaries, ovaries, testes and kidneys (Anbar *et al.*, 1959; Perlman *et al.*, 1941; Durand, 1938). The tissue to plasma iodide ratio is greatest in the thyroid. The thyroid's ability to concentrate iodide is necessary for the process of thyroid hormones synthesis.

Iodide is actively transferred into the thyroid by the sodium-iodide symporter (NIS), a protein that resides in the basolateral membrane of thyroid epithelial cells. Abnormalities in expression or function of the symporter can lead to thyroid disease (Spitzweg *et al.*, 2000). The NIS simultaneously transports both Na^+ and I^- ions from extracellular fluid (plasma) into the thyroid epithelial cell. This process is an example of secondary active transport. Energy is provided by the electrochemical gradient of sodium across the cell membrane; the low intracellular concentration of sodium is maintained by sodium-potassium pumps (Ajjan *et al.*, 1998).

The presence of NIS is an indicator of active uptake for iodide. NIS is highly expressed in thyroid epithelial cells. Lower levels of expression have been detected in the mammary gland, salivary gland, skin, stomach and colon (Ajjan *et al.*, 1998; Spitzweg *et al.*, 1998). However, only the thyroid has been found to organify iodide (Ajjan *et al.*, 1998). The most important regulator of symporter gene and protein expression is thyroid-stimulating hormone (TSH). This is also the case for other important thyroid proteins such as thyroglobulin and thyroid peroxidase (Spitzweg *et al.*, 1998).

The proposed PBPK model describes active uptake of iodide and perchlorate in gastric juice, thyroid and skin, competitive inhibition of iodide uptake by perchlorate in NIS-containing tissues, as well as venous equilibration with slowly and richly perfused tissues. Perchlorate's transport mechanisms can be modeled similarly to that of iodide, as it binds to the NIS and competitively inhibits iodide uptake (Anbar *et al.*, 1959; Brown-Grant and Pethes, 1959). The kinetics of these anions differ mainly in that iodide is organified in the thyroid (thyroid hormone

production) whereas perchlorate is thought to be unreactive and eventually diffuses from the thyroid into systemic circulation. Although perchlorate is quickly eliminated unchanged in the urine (Wolff, 1998), understanding the impact of chronic displacement of iodide from prolonged exposure to perchlorate-contaminated drinking water is the focus of this and other ongoing modeling efforts.

The objective of this effort is to develop a PBPK model for use in the simulation of serum perchlorate and iodide levels and the subsequent inhibition of iodide uptake into the thyroid. This PBPK model is fitted to experimental data collected in house, as well as literature data using substantiated parameter values. The model structure does not include effects of chronic perchlorate exposure on thyroid hormone homeostasis at this point.

METHODS

Chemicals. Ammonium perchlorate (99.9% purity), trichloroacetic acid and sodium iodide were purchased from Aldrich Co. (St. Louis, MO), and carrier free radiolabeled iodide ($^{125}I^-$) from Amersham Pharmacia Biotech (Piscataway, NJ). Sodium hydroxide was obtained from Fisher Scientific (Fairlawn, NJ) and HPLC grade ethanol from Sigma Chemicals (St. Louis, MO). The water used in the study was treated by a reverse osmosis system and then deionized. Carrier-free $^{125}I^-$ (specific activity 16.0-17.4 mCi/μg) was purchased from Amersham Pharmaceutical Biotech (Piscataway, NJ). Radiolabeled perchlorate ($^{36}ClO_4^-$; specific activity 493.2 mCi/mole) was custom-made by New England Nuclear (N. Billerica, MA).

Animals. Male Sprague-Dawley rats (330 ± 35g, n=6 rats per group) were purchased from Charles River Laboratories (Raleigh, NC) and housed in laminar airflow enclosures with 12hr:12hr light:dark cycles. Rats were provided Purina lab chow and water *ad libitium*. Rats used for urine collection were individually placed in metabolism cages; water and powdered food were freely available.

Unless mentioned otherwise, intravenous dosing was carried out via lateral tail vein injection (volume = 0.67 mL/kg) while controls received 0.67 mL/kg of physiological saline. Procedures (*iv* administration and euthanization of rats by CO_2 asphyxiation) were scheduled for mornings (5:30-11:30 AM). Tissues were harvested, weighed and kept at -20°C.

For the following experiments, the term total iodine includes bound iodine plus free inorganic iodide. Carrier doses included tracer doses of carrier free $^{125}I^-$ along with non-radiolabeled iodide. Free $^{125}I^-$ radioactivity was determined by subtracting the bound from total measurements.

Acute *iv* Kinetics Experiments:

Radiolabeled iodide ($^{125}I^-$) kinetics: Male rats were administered a single *iv* tail vein injection with physiological saline (control group) or 33 µg/kg $^{125}I^-$ (with carrier) in physiological saline. Rats were euthanized by CO_2 asphyxiation at 5, 15 and 30 minutes (min), 1, 2, 6, 9, 24, 32, 48 and 96 hours (h) post dosing to collect thyroid and blood from the vena cava. Rats for the 24 hour time point were placed individually in metabolism cages to collect urine.

In an additional study, male rats were intravenously dosed with 33 µg/kg $^{125}I^-$ (with carrier) and euthanized at 0.5, 2 and 6 hours post dosing. Total, bound and free $^{125}I^-$ were analyzed in thyroid and serum, and total $^{125}I^-$ in skin and gastric contents.

Radiolabeled $^{36}ClO_4^-$ kinetics: Naïve male Sprague-Dawley rats (300 ± 20 g) were dosed once by intravenous tail vein injection with 3.3 mg/kg radiolabeled perchlorate. Due to the low specific activity, a smaller dosing level could not be achieved. Each rat received less than 6 µCi. Rats were euthanized by CO_2 asphyxiation at 0.5, 6, 12, 24, 32 and 48 hours after dosing. The thyroid, intestinal tract, intestinal tract contents, muscle, skin, liver, kidney, spleen, bladder, plasma and red blood cells were harvested from the rats and stored at -20°C until analysis of $^{36}ClO_4^-$. Rats for 12, 24, 32 and 48 hours time points were placed individually in metabolism cages for urine collection. Metabolism cages were washed with 500 mL de-ionized water. Urine and cage wash samples were stored under the same conditions until analysis.

$^{125}I^-$ Kinetics and Inhibition from Acute *iv* Dosing with ClO_4^-: Rats were injected with one of five doses of perchlorate (0.0, 0.01, 0.1, 1.0 and 3.0 mg/kg). At 2 hours post dosing, they were challenged with $^{125}I^-$ with carrier (33 µg/kg) by intravenous injection and euthanized at 5, 15 and 30 min, 1, 2, 6, 9 and 24 hours post dosing of iodide. This corresponds to 2.08, 2.25, 2.5, 3, 4, 8, 11 and 26 hours, respectively, after dosing with perchlorate. Blood and thyroid were harvested from all time point groups; urine was collected from rats in the 24 hours dose group. Perchlorate and iodide levels were determined in the thyroid, serum and urine.

In an additional study, three rats were intravenously dosed with 0.0, 0.1 and 1.0 mg/kg perchlorate and challenged two hours later with 33 µg/kg $^{125}I^-$. Rats were euthanized at 15 min, 1, 2, and 4 hours after they were dosed with iodide. Levels of perchlorate and $^{125}I^-$ were determined in thyroid, serum, skin and gastric contents.

Drinking Water Studies

Inhibition of Thyroid $^{125}I^-$ Uptake (with carrier) after Drinking Water Exposure to ClO_4^-: To investigate the inhibitory effects of perchlorate, three drinking water studies (1, 5 and 14 days) were performed with target perchlorate concentrations of 0.0, 1.0, 3.0, 10.0 and 30.0

mg/kg-day with male rats continually exposed via drinking water. At the end of day 1, 5 or 14, rats (n=6 per group) were challenged once with 33 μg/kg $^{125}I^-$ with carrier and euthanized at 2 hours post iodide dosing. Blood and thyroid gland were collected for ClO_4^- and $^{125}I^-$ analyses in serum. For the 10 and 30 mg/kg dose groups, perchlorate was measured in serum and thyroid on day 5; however the iodide inhibition study for these dose groups was conducted on Day 14.

Analytical Methods

$^{125}I^-$ with Carrier Analysis in Tissues: Thyroid lobes were weighed and one or two lobes were placed in a 0.2 mL-micro tissue homogenizer (Kontes Glass Co., Vineland, NJ) and homogenized with 100 μL of water. Thyroid homogenate was transferred into a polystyrene, round bottom tube (12 mm x 75 mm). The micro tissue homogenizer was washed three times with 120 μL of water to ensure complete transfer of the homogenate. Total radioactivity of the thyroid homogenate was counted by a γ-counter (Packard Instrument Co., Meriden, CT). Half a milliliter of 10% trichloroacetic acid (TCA) was then added to precipitate proteins. The homogenate was vortexed for 2 to 3 seconds, centrifuged for 10 min at 5000 rpm, and the supernatant was transferred into a polystyrene tube. Half a milliliter of 5% TCA was added to the pellet. The pellet was gently dislodged and shaken. The mixture was centrifuged and decanted as above. Using half a milliliter of 2.5% TCA, the centrifuge procedure was again repeated. Radioactivity of the supernatant (free) and the pellet (bound) was measured by a γ-counter.

Aliquots of serum or urine were placed into a round polystyrene tube and total radioactivity was determined by a γ-counter. Free and bound radioactivity measurements of serum or urine were carried out in the same manner as described for thyroid homogenate.

High Pressure Liquid Chromatography (HPLC) Analysis of Perchlorate: Thyroid specimens from control and perchlorate dosed rats were homogenized in 250 μL of deionized water in a micro tissue homogenizer. Homogenates were centrifuged at 31,500 x G for 30 min at 4°C. The supernatants were diluted 10, 25, 50 and 100 times with water, bringing the final volume to 2 mL. The diluted supernatants were filtered through 0.45 μm non-sterile acrodisc syringe filters with Versapor (supported acrylic copolymer) membranes (Pall Gelmann Laboratory, Ann Arbor, MI). One mL of each filtrate was injected into the HPLC system using an autosampler.

Perchlorate analyses of serum and urine samples were carried out by mixing 100 μL samples with 300 μL ice-cold ethanol. The mixture was centrifuged at 31,500 x G for 30 min at 4°C. Supernatants were evaporated to dryness under nitrogen at 37°C and reconstituted in 2 mL of water. Reconstituted serum and urine samples were filtered as above for thyroid samples. One mL of each filtrate was injected into the HPLC.

HPLC Conditions: Analyses were performed with a Model Dx-300 liquid chromatographic system equipped with a background conductivity suppressor (Dionex, Sunnyvale, CA). The system consists of an advanced gradient pump (AGP standard size), conductivity detector (CDM-3), an anion self regenerating suppressor (ASRS 4mm) for the reduction of background conductivity of the eluent, an autosampler (AS-3500), a 1000 μL sample loop, a computer interface (ACI) and software (Autolon 450). Separation by isocratic elution of perchlorate was performed on a Dionex AS11 analytical column (4 x 250 mm) preceded by a Dionex AG 11 guard column (4 x 50 mm). The sensitivity of the detector was maintained between 0.5 and 100 μS depending on the concentration. The mobile phase (flow rate = 1 mL) was 100 mM sodium hydroxide in water. The mobile phase was filtered through a 0.45 μm filter with a nylon membrane (Micron Separations Inc., Westboro, MA) and degassed under vacuum before use. Perchlorate standards were prepared in water in the range of 0.5 to 100 ng/mL.

Analysis of TSH and Thyroid Hormones

The hormone assays were conducted using radio-immunoassay (RIA) kits following the manufacturers' instructions. Kits for T_4, free T_4 and T_3 were purchased from Diagnostic Product Corp. (Los Angeles, CA) and kits for TSH from Amersham Corp. (Arlington Heights, IL). Standards and samples were run in triplicate and assay kits from the same batch number and with the same expiration date were used for all thyroid hormones or TSH measurements for each animal. Tracer $^{125}I^-$ activity was measured with a γ-counter.

Model Structure

Based on the similar ionic size of iodide and perchlorate and a shared affinity for NIS, the same model structure was used to describe the distribution of both anions (Figure 1). Tissues that exhibited evidence of sodium iodide symporter and were found to concentrate either anion, were depicted as compartments with nonlinear uptake. Tissues with active uptake include the thyroid, skin and gastric mucosa (Wolff, 1998; Chow *et al.*, 1969; Kotani *et al.*, 1998). Although other tissues have been known to sequester iodide and similar anions (e.g., salivary glands, choroid plexus, ovaries, mammary glands, placenta) (Brown-Grant, 1961, Honour *et al.*, 1952; Spitzweg *et al.*, 1998), the iodide and perchlorate pools of these tissues are expected to be too small to significantly affect plasma levels. These tissues were lumped with slowly and richly perfused tissues.

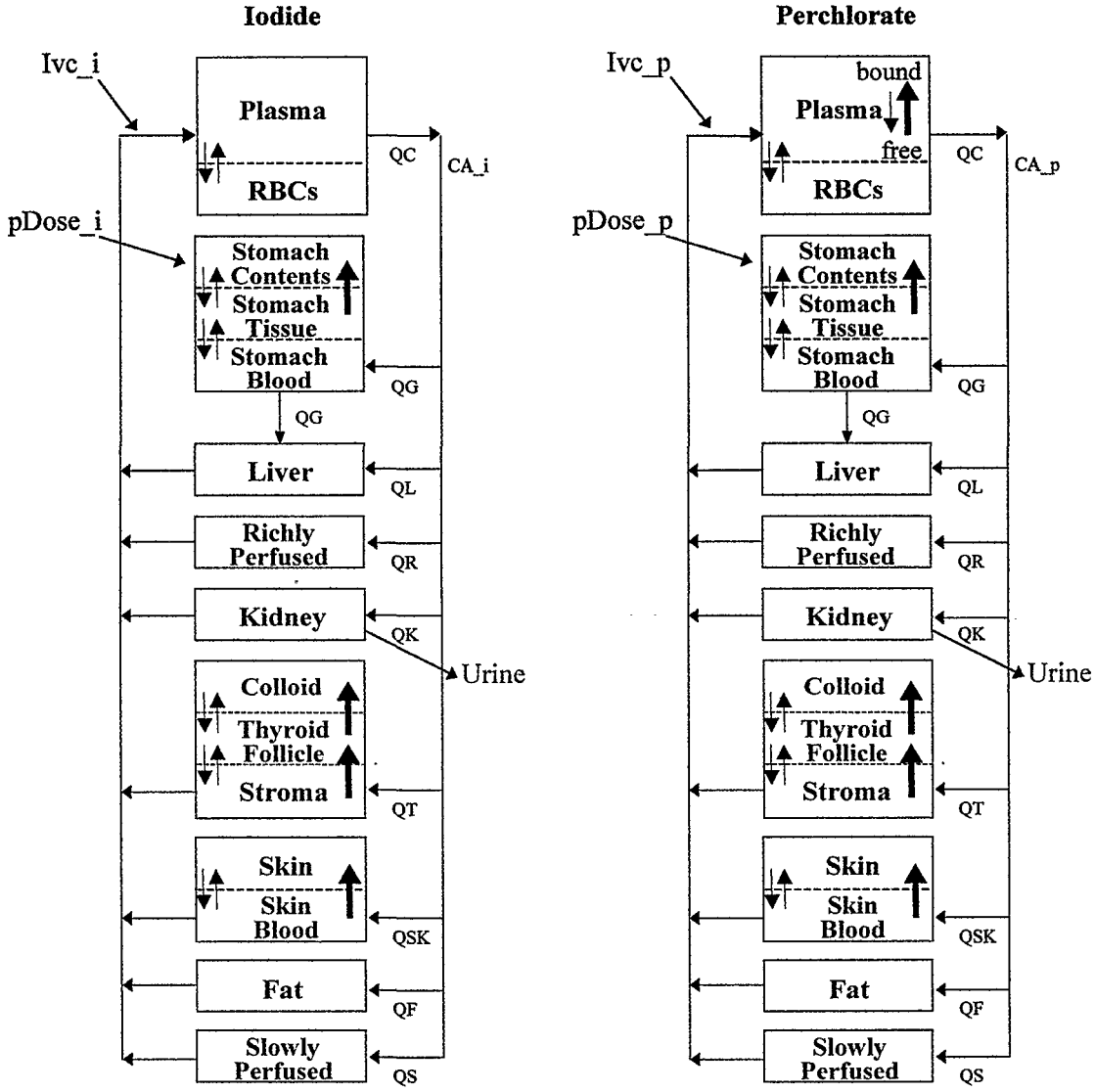

Figure 1. Schematic of PBPK model for perchlorate and iodide distribution. Bold arrows indicate active uptake at NIS sites (with exception plasma binding). Small arrows indicate passive diffusion.

In addition to the thyroid, stomach, skin, slowly and richly perfused compartments, the model also includes separate compartments for plasma, kidney, liver and fat. The stomach and thyroid consist of three sub-compartments representing the stroma, the follicle and the colloid in the thyroid, or the capillary bed, stomach wall and contents in the case of the stomach. The skin contains two sub-compartments representing the capillary bed and the skin tissue. Active uptake into the thyroid colloid, stomach contents and skin were described using Michealis-Menten kinetics for nonlinear processes (Figure 1, bold arrows). Permeability area cross products and partition coefficients were used to describe the first order movement of the anions (ClO_4^- and I-) between the capillary bed, tissue and inner (deep) compartments (Figure 1, small arrows), which

results from the inherent electrochemical gradient within the tissues. Passive diffusion through the kidney, liver and fat compartments were described with partitions and blood flows. Plasma binding of perchlorate was described with Michealis-Menten terms for the association of the ClO_4^- anions to plasma binding sites and a first order clearance rate for the dissociation. First order clearance rates from the kidney were also used to describe urinary clearance of the anions.

Few studies have measured perchlorate or iodide in skin. Our laboratory reported $^{36}ClO_4^-$ in male rat skin at higher concentrations than in plasma for several hours after *iv* adminstration (Fisher *et al.*, 2000). Zeghal *et al.* (1995) examined the effects of perchlorate on the iodine composition of rat skin. Although Zeghal and his colleagues did not measure skin perchlorate levels directly, they reported a significant reduction in skin iodide in young and adult rats after its administration, suggesting competitive inhibition.

Iodide has also been reported in the skin at higher concentrations than in plasma after *iv* dosing but results have not been consistent. Brown-Grant and Pethes (1959) observed skin:serum ratios as high as 2.0 in adult male rats and 6.0 in young pups. The skin:serum ratio was higher in the adult male than female rats. Brown-Grant and Pethes did not find this to occur in guinea pigs or mice. Our *in vivo* studies with radioiodide in rats resulted in skin:serum iodide ratios near one (Yu *et al.*, 2000a), while Perlman *et al.* (1941) reported skin:plasma iodide ratios in rabbits less than one (0.6 to 0.7). NIS expression has been reported in rat skin (Kotani *et al.*, 1998). Therefore, it is possible that the kinetics of perchlorate and iodide in skin are similar.

Behavior similar to that of iodide in skin has been seen in pertechnetate (an anion with a shared affinity for NIS). Hays and Green (1973) performed dialysis studies on intact human tissues with pertechnetate. They found skin had a relatively slow uptake, peaking at 18 hours, and had some retention after leaching dialysis, in fact more retention than brain, muscle and serum. Due to its significant percentage of body weight, the skin represents an important pool for slow iodide turnover and therefore was maintained as a separate compartment in the model.

The kidney, liver and fat do not maintain concentrations greater than the plasma and therefore do not contain terms for active uptake. The rapid urinary clearance of perchlorate required inclusion of a kidney. The liver compartment was included since the majority of extrathyroidal deiodination takes place there. Although the model does not currently include hormone production or deiodination, the future development of the model will require a liver compartment. Fat does not absorb iodide or perchlorate well. However, wide variation in fat content of human populations could alter perchlorate/iodide kinetics. Therefore, for the purpose of using the model for species extrapolations, fat is included in the model as an exclusionary compartment.

The blood compartment differs between the perchlorate and iodide models. The perchlorate blood compartment is composed of plasma and plasma proteins to simulate binding. Plasma binding was required to simulate serum perchlorate concentrations at lower doses. Iodinated hormones bind to plasma proteins, but free iodide apparently does not; therefore a single compartment for plasma iodide is used. The free anions in plasma are available for diffusion and active uptake into tissues.

Shishiba *et al.* (1970) studied the effect of perchlorate on the free thyroxine (fT_4) fraction in human blood. They found that perchlorate interfered with the binding of fT_4 to prealbumin and albumin, but not thyroglobulin (TBG). Yamada (1967) reported an increased fT_4 fraction in rat blood after administration of perchlorate. While they found perchlorate to have a greater effect than thiocyanate (SCN^-) in rats, Shishiba found perchlorate to have less effect in human blood. These studies suggest a species difference in protein/perchlorate interaction in the blood. Studies performed by Hays and Green (1973) on pertechnetate found that perchlorate blocked the binding of pertechnetate to human serum albumin.

Carr (1952) measured perchlorate binding in bovine albumin. He found that perchlorate bound to nearly the same extent as thiocyanate (SCN^-). Perchlorate binding in human serum was measured by Scatchard and Black (1949). Their studies also revealed that perchlorate binding was very similar to that of SCN^-, both anions exhibiting reversible binding to human albumin via weak covalent interactions. This binding, although not measured directly in the rat, is evidenced through the displacement of T_4 in rat serum. Given that perchlorate demonstrates a similar or slightly smaller ability to bind to albumin or prealbumin in human serum, it is feasible to assume from Shishiba's studies, that perchlorate is bound to a greater extent in rat serum. This is also supported by the fact that thyroxine is primarily transported by albumin in rats as opposed to TBG in humans, which was shown not to be affected by perchlorate. Thus, is it reasonable to assume that protein binding would have a greater effect on the distribution and clearance of the anion in the rat as opposed to the human.

Physiological Parameters

Rat tissue volumes and blood flows were obtained from the literature or our in-house kinetic studies (Table 1).

Table 1. Physiological Parameters for the Male Rat

Tissue Volumes	Male Rat	Source
Body Weight BW (kg)	0.3	Measured (rat specific)
Slowly Perfused VSc (%BW)	74.6	Brown *et al.*, 1997
Richly Perfused VRc (%BW)	11.0	Brown *et al.*, 1997
Fat VFc (%BW)	7.4	Brown *et al.*, 1997
Kidney VKc (%BW)	1.7	Brown *et al.*, 1997
Liver VLc (%BW)	5.5	Brown *et al.*, 1997
Stomach Tissue VGc (%BW)	0.54	In house male rat ClO_4^- kinetics (Yu *et al.*, 2000a)
Gastric Juice VGJc (%BW)	1.68	In house male rat ClO_4^- kinetics (Yu *et al.*, 2000a)
Stomach Blood VGBc (%VG)	4.1	Altman & Dittmer, 1971b
Skin Tissue VSkc (%BW)	19.0	Brown *et al.*, 1997
Skin Blood VSkBc (%VSk)	2.0	Brown *et al.*, 1997
Thyroid Vttotc (%BW)	0.0077	Malendowicz, 1977
Thyroid Follicle VTc (%Vttot)	59.9	Malendowicz, 1977
Thyroid Colloid VDTc (%VTtot)	24.4	Malendowicz, 1977
Thyroid Blood VTBc (%VTtot)	15.7	Malendowicz, 1977
Plasma Vplasc (%BW)	4.1	Brown *et al.*, 1997, Altman & Dittmer, 1971a
Red Blood Cells VRBCc (%BW)	3.3	Brown *et al.*, 1997, Altman & Dittmer, 1971a
Adjusted Slowly Perfused VS (L)	0.138	Calculated from model
Adjusted Richly Perfused VR (L)	0.01	Calculated from model
Blood Flows		
Cardiac Output QCc (L/h/kg)	14.0	Brown *et al.*, 1997, Hanwell & Linzell, 1973
Slowly Perfused QSc (%QC)	24.0	Brown *et al.*, 1997
Richly Perfused QRc (%QC)	76.0	Brown *et al.*, 1997
Fat QFc (%QC)	6.9	Brown *et al.*, 1997
Kidney QKc (%QC)	14.0	Brown *et al.*, 1997
Liver QLc (%QC)	17.0	Brown *et al.*, 1997
Stomach QGc (%QC)	1.61	Malik *et al.*, 1976
Skin QSkc (%QC)	5.8	Brown *et al.*, 1997
Thyroid QTc (%QC)	1.6	Brown *et al.*, 1997
Adjusted Slowly Perfused QS (%QC)	11.3	Calculated from model
Adjusted Richly Perfused QR (%QC)	41.8	Calculated from model

Partitioning Coefficients

Steady state values from infusion studies were not available for either anion. Therefore, partition coefficients for iodide and perchlorate were estimated from *in vivo* studies (Table 2). Halmi *et al.* (1956) measured organ to serum concentration ratios for radioiodide in rats approximately 1, 4 and 24 hours after an *iv* dose of the tracer iodide. The average liver:serum and muscle:serum iodide ratios at approximately four hours after an injection of $^{131}I^-$ (0.40 and 0.21, respectively) were used to represent richly and slowly perfused partitioning coefficients for iodide. Perlman *et al.* (1941) reported similar iodine ratios in rabbit tissues five hours after subcutaneous dosing with NaCl and a tracer amount of iodide (0.44 for liver/blood and 0.19 for muscle/blood). The liver:blood and muscle:blood, ratios reported by Perlman remained relatively constant for up to 96 hours. A value of 0.05 was reported for the partitioning of perchlorate into the fat of a hen

(Pena *et al.*, 1976). This value was also used to represent iodide partitioning into fat in our model.

Due to a lack of information on perchlorate distribution, several partition coefficients for perchlorate were derived from the $^{36}ClO_4^-$ kinetic study described above. Twenty-four hours after a single *iv* dose of 3.3 mg $^{36}ClO_4^-$/kg, the liver:serum and muscle:serum ratios were 0.56 and 0.31, respectively. These values were used to represent slowly perfused tissue (0.31), liver (0.56) and richly perfused tissue (0.56). Anbar *et al.* (1959) reported similar liver:blood and muscle:blood ratios of 0.38 and 0.12, respectively, in rabbits 12 hours after an intraperiteneal (*ip*) dose of 100 mg $KClO_4$.

For compartments with nonlinear uptake of the anions, effective partition coefficients were used, representing either approximate tissue:serum concentrations ratios or electrical potential gradients. The effective partition coefficients for iodide in the stomach compartments were also derived from in-house experiments. Stomach wall:serum and gastric juice:stomach wall perchlorate ratios of 1.8 and 2.3, respectively, were derived 24 hours after the *iv* dose. The corresponding stomach iodide partitions, derived from in-house $^{125}I^-$ kinetic studies, were 0.5 for the stomach tissue:serum and 3.5 for the gastric juice:stomach (Yu *et al.*, 2000b).

Skin measurements from the in-house $^{36}ClO_4^-$ kinetic study were highly variable and suggested an effective partitioning greater than one. Based on the 24 hour timepoint, an effective partition coefficient of 1.15 was derived. Our acute $^{125}I^-$ data suggest its effective partition in skin was less than one. The iodide value used (0.7) was derived from Perlman *et al.* (1941). He reported skin:plasma iodide ratios from 0.6 to 0.7 in rabbits, 6 to 96 hours after a subcutaneous dose of tracer radioiodide.

Chow and Woodbury (1970) measured electrochemical potentials within the thyroid stroma, follicular membrane and colloid at three different doses of ClO_4^-. Their measured difference in electrical potential between the thyroid stroma and follicle can be interpreted as an effective partition coefficient for charged moieties, such as ClO_4^- and I^-, hindering the entry of negatively charged ions into the follicle. The equal and opposite potential from the follicle to the colloid enhances passage of negatively charged species into the colloid, and indicates an effective partition coefficient of greater than one.

The equivalence between electrical potential differences ϕ_i - ϕ_o and effective partition coefficients can be estimated in the manner of Kotyk and Janacek (1977) as follows:

$$\phi_i - \phi_o = 2.303 \frac{RT}{zF} \log \frac{c_o}{c_i}$$

where R is the gas constant, T is the absolute temperature and F is the Faraday constant. At 37°C, 2.303RT/F = 61.6 mV, so for a singly charged ion (z=1), this becomes:

$$\phi_i - \phi_o = 61.6 \log \frac{c_o}{c_i} \quad \text{(mV)}$$

In general, the ratio of a species concentrations between two media is given by the partition coefficient (K_p), where $K_p = c_o/c_i$. Thus, the previous equation becomes:

$$\phi_i - \phi_o = 61.6 \log K_p$$

or

$$K_p = 10^{\phi_i - \phi_o / 61.6}$$

From Chow and Woodbury (1970), the potential difference for the stroma:follicle interface ranges from –58 to –51 mV. Therefore, from the above equation, K_p for a monovalent, negatively charged ion is between 0.114 and 0.149. Similarly, for the follicle:lumen interface, $\phi_i - \phi_o$ ranges from +50 to +58 mV, rendering the effective K_p between 6.48 and 8.74. These values were also used to describe the uptake of iodide due to the electrochemical gradient, based on the fact that iodide and perchlorate have the same ionic charge.

Table 2. Chemical Specific Parameters for Male Rat Model

Partition Coefficients (unitless)[a]	Perchlorate	Iodide	Source
Slowly Perfused / Plasma PS_	0.31	0.21	Yu *et al.*, 2000a; Halmi *et al.*, 1956
Richly Perfused / Plasma PR_	0.56	0.40	Yu *et al.*, 2000a; Halmi *et al.*, 1956
Fat/ Plasma PF_	0.05	0.05	Pena *et al.*, 1976
Kidney/ Plasma PK_	0.99	1.09	Perlman *et al.*, 1941
Liver/Plasma PL_	0.56	0.44	Perlman *et al.*, 1941
Gastric Tissue/Gastric Blood PG_	1.80	0.50	Yu *et al.*, 2000a;Yu *et al.*, 2000b
Gastric Juice/Gastric Tissue PGJ_	2.30	3.50	Yu *et al.*, 2000a; Yu *et al.*, 2000b
Skin Tissue/Skin Blood PSk_	1.15	0.70	Yu *et al.*, 2000b, Perlman *et al.*, 1941
Thyroid Tissue/Thyroid Blood PT_	0.13	0.15	Chow & Woodbury (1970)
Thyroid Lumen/Thyroid Tissue PDT_	7.00	7.00	Chow & Woodbury (1970)
Red Blood Cells/Plasma	0.80	1.00	Yu *et al.*, 2000a; Rall *et al.*, 1950
Max Capacity, Vmaxc (ng/h/kg)			
Thyroid Colloid Vmaxc_DT	1.0E+04	4.0E+07	Fitted
Thyroid Follicle Vmaxc_T	2.2E+03	5.5E+04	Fitted
Skin Vmaxc_S	6.2E+05	5.0E+05	Fitted
Gut Vmaxc_G	1.0E+04	2.0E+06	Fitted
Affinity Constants, Km (ng/L)			
Thyroid Lumen Km_DT	1.0E+08	1.0E+09	Golstein *et al.*, 1992
Thyroid Km_T	2.5E+05	4.0E+06	Gluzman & Niepomniszcze, 1983; Wolff, 1998
Skin Km_S	2.0E+05	4.0E+06	Gluzman & Niepomniszcze, 1983; Wolff, 1998
Gut Km_G	2.0E+05	4.0E+06	Gluzman & Niepomniszcze, 1983; Wolff, 1998
Plasma binding Km_B	1.1E+04	---	Fitted
Permeability Area Cross Products, (L/h-kg)			
Gastric Blood to Gastric Tissue PAGc_	0.80	1.00	Fitted
Gastric Tissue to Gastric Juice PAGJc_	0.80	0.10	Fitted
Skin Blood to Skin Tissue PASkc_	1.0	0.10	Fitted
Plasma to Red Blood Cells PARBCc_	0.10	1.00	Fitted
Follicle to thyroid blood PATc_	4.0E-05	1.0E-04	Fitted
Lumen to Thyroid Follicle PADTc_	0.01	1.0E-04	Fitted
Clearance Values, (L/h-kg)	---		
Urinary excretion CLUc_	0.07	0.05	Fitted
Plasma unbinding Clunbc__	0.1	---	Fitted

Notes:

a. All parameters listed are notated in the model by either an *i* (for iodide) or *p* (for perchlorate) following the parameter name (e.g., *PR_i, PR_p, Vmaxc_Ti, Vmaxc_Tp, etc.*).

Affinity Constants and Maximum Velocities

Wolff (1998) noted that iodide's Km for NIS is similar in different tissues . Gluzman and Niepomniszcze (1983) derived a mean Michealis-Menten affinity constant (Km) of 3.96 x 10^6 ng/L for iodide from thyroid slices of 5 normal individuals. The thyroid slices were incubated with several medium iodide concentrations. The authors noted little variation between normal and pathological human thyroid specimens, or between thyroid specimens of different species. Therefore, a Km value of 4.0 x 10^6 ng/L was assumed to describe the affinity of iodide across compartments involving active uptake by NIS (thyroid and gastric juices).

Wolff also noted that the Km for perchlorate and other similar monovalent anions decreased with the anions' ability to inhibit iodide uptake. The molar equivalent of iodide's Km for perchlorate

is 3.1 x 10^6 ng/L. Several studies suggest perchlorate is a more potent inhibitor than iodide. In the rat thyroid, Wyngaarden *et al.* (1952) have shown that perchlorate was a more powerful inhibitor of the iodide trap than thiocyanate. Halmi and Stuelke (1959) showed that perchlorate was ten times as effective as iodide in depressing tissue to blood ratios in the rat thyroid and gut. Similarly, Harden *et al.* (1968) compared human saliva to plasma radioiodide concentration ratios after equimolar doses of perchlorate and iodide. The saliva/plasma iodide ratios, during resting conditions, were approximately seven times lower after a molar equivalent dose of perchlorate vs. iodide. Lazarus *et al.* (1974) also demonstrated that perchlorate was taken up to greater extent in mice salivary glands than iodide. Based on this information, a Km between 2.0 x 10^5 and 2.5 x 10^5 ng/L, approximately 10 times lower than that of iodide, was estimated to represent perchlorate's affinity for NIS.

The apical follicular membrane also exhibits a selective iodide uptake mechanism. Golstein *et al.* (1992) found the affinity for iodide transport from the bovine thyroid follicle into the colloid (Km_DTp) to be approximately 4.0 x 10^9 ng/L. This iodide channel also appears to be very sensitive to perchlorate inhibition and shares a similar permeability to perchlorate as to iodide. The ability of perchlorate to inhibit iodide uptake at the apical follicular membrane suggests that the Km of perchlorate at the apical follicular membrane (Km_Dtp) is also lower than that of iodide. Model simulations of thyroid inhibition supported a value of 1.0 x 10^8 ng/L, approximately ten times less than that of iodide.

Whereas the Km is similar across tissues containing NIS, the maximum velocity term (Vmax) does vary between tissues and species (Wolff, 1998), being lower in humans than other species (Gluzman and Niepomniszcze, 1983; Wolff and Maurey, 1961). Maximum velocities or capacities (Vmaxc) were not found in the literature and were therefore estimated for a given compartment by fitting the simulation to the data at varying doses (Table 2).

TSH increases the total amount of carrier in a membrane, thereby increasing the thyroid Vmax. This TSH effect does not occur in other tissues with active uptake and appears to be unique to the thyroid NIS. The up-regulation of NIS protein expression in mammary glands of lactating rats during suckling may be regulated by prolactin and/or oxytocin (Spitzweg *et al.*, 2000), suggesting other agents may stimulate NIS expression and function. In addition to hyper- or hypo-stimulation of trapping activity by TSH, the intrathyroidal iodide pool and the magnitude of iodide efflux are also responsible for variations in Vmax (Bagchi and Fawcett, 1973). Currently the iodide model does not account for TSH stimulation and endogenous iodide pools.

Fitting Model Parameters to Observed Data

Parameter terminology used in this model is summarized in Table 2. Simultaneous differential equations, which simulate radioiodide and perchlorate distribution in the proposed mathematical model, were written and solved using ACSL (Advanced Continuous Simulation Language) software (AEgis Technologies, Austin, TX).

Permeability Area Cross Products and Clearance Values

Permeability area cross products (PA) and partition coefficients (P) were used to describe diffusion limited uptake in tissues requiring subcompartments. The PA values in this model were fitted by setting the partition coefficients to the literature values in Table 2. The equations below illustrate the use of PA's:

$$RAXB\_y = QX \times (CA\_y - CVXB\_y) + PAX\_y \times \left(CX\_y / PX\_y - CVXB\_y \right)$$

$$AXB\_y = Integ(RAXB\_y, 0.0)$$

$$CVXB = AXB / VXB$$

$$RAX\_y = PAX\_y \times \left(CVXB\_y - CX\_y / PX\_y \right)$$

$$AX\_y = Integ(RAX\_y, 0.0)$$

$$CX = AX / VX$$

where:

RAXB_y =	Rate of clearance of y^{th} anion from X^{th} tissue's capillary bed (ng/h)
QX =	Blood flow through X^{th} tissue (L/h)
CA_y =	Arterial blood concentration of y^{th} anion (ng/L)
CVXB_y =	Venous blood concentration of y^{th} anion (ng/L)
CX_y =	Tissue concentration of y^{th} anion (ng/L)
AXB_y =	Amount of y^{th} anion in tissue's capillary bed.

Fitted clearance values were used to describe first order urinary excretion rates and reversible plasma binding to serum, as shown below:

$$RAX = CX\_y \times ClX\_y$$

where:

RAX = rate of clearance from X^{th} compartment (ng/h)
CX_y = concentration of y^{th} anion within X^{th} compartment (ng/L)
ClX_y = clearance value of y^{th} anion into X^{th} compartment (L/h)

Saturable Processes

The basic equation used to simulate active uptake of iodide and perchlorate alone (without accounting for inhibition) in tissues with NIS activity is:

$$\frac{dAX\_y}{dt} = \frac{V\max\_Xy \times CVX\_y}{Km\_Xy + CVX\_y}$$

where:

AX_y = Amount of y^{th} anion in X^{th} tissue (ng)
t = Time
Vmax_Xy = Maximum uptake of y^{th} anion at X^{th} tissue's symporter (ng/h)

Km_Xy = Michaelis-Menton affinity constant for y^{th} anion in X^{th} compartment (ng/L)
CVX_y = Concentration of y^{th} anion in capillary blood of X^{th} compartment (ng/L)

Accounting for inhibition of active uptake of either iodide or perchlorate in the presence of the competing anion is expressed as:

$$\frac{dAX\_y}{dt} = \frac{V\max\_Xy \times CVX\_y}{Km\_Xy \times \left(1 + {}^{CVX\_z}/_{Km\_Xz}\right) + CVX\_y}$$

where:
Km_Xz = M-M affinity constant for z^{th} anion (competitive inhibitor) in X^{th} compartment (ng/L)
CVX_y = Concentration of z^{th} anion (competitive inhibitor) in venous capillary blood of X^{th} compartment (ng/L)

Example equations for simulating the transport of iodide through the thyroid are provided below. The equations include blood flow through the thyroid capillary bed (stroma) as well as active uptake and inhibition by perchlorate in both the follicle and colloid.

- Rate of change in thyroid blood (*RATB_i*)

$$RATB\_i = QT \times (CA\_i - CVTB\_i) + PAT\_i \times \left({}^{CT\_i}/_{PT\_i - CVTB\_i}\right) - RupT\_i$$

- Rate of change in follicle (*RAT_i*)

$$RAT\_i = RupT\_i + PAT\_i \times \left({}^{CVTB\_i - CT\_i}/_{PT\_i}\right) - RupDT\_i + PADT\_i \times \left({}^{CDT\_i}/_{PDT\_i - CT\_i}\right)$$

- Rate of change in Colloid (*RADT_i*)

$$RADT\_i = RupDT\_i + PADT\_i \times \left({}^{CT\_i - CDT\_i}/_{PDT\_i}\right)$$

- Rate of active uptake in the follicle (*RupT_i*) with inhibition

$$RupT\_i = \frac{V\max\_Ti \times CVTB\_i}{Km\_Ti \times \left(1 + {}^{CVTB\_p}/_{Km\_Tp}\right) + CVT\_i}$$

- Rate of active uptake into the colloid (*RupDT_i*) with inhibition

$$RupDT\_i = \frac{V\max\_DTi \times CT\_i}{Km\_DTi \times \left(1 + {}^{CT\_p}/_{Km\_DTp}\right) + CT\_i}$$

Allometric Scaling

To account for parameter differences due to varying body weights of rats and humans, allometric scaling was utilized. The following equations provide the allometric scaling applied to the

maximum velocity (Vmax), permeability area cross products (PA), clearance values (Cl), tissue volumes (V) and blood flows (Q).

$$V\max\_Xi = V\max c\_Xi \times BW^{3/4}$$
$$PAX\_i = PAXc\_i \times BW^{3/4}$$
$$ClX\_y = ClXc\_y \times BW^{3/4}$$
$$QC = QCc \times BW^{3/4}$$
$$VX = VXc \times BW$$

where:

"c" following the parameter name indicates the value of the constant before allometric scaling

"X" represents the tissue (or lumped compartment) of interest.

"y" indicates anion of concern (i.e, i = iodide, p = perchlorate)

RESULTS AND DISCUSSION

Parameterization of ClO_4^- Model

The resulting simulations of various tissues and serum concentrations were derived using the physiological and chemical specific parameters provided in Tables 1 and 2. Figures 2A through I illustrate the model predictions of kinetic data after acute $^{36}ClO_4^-$ *iv* dosing. The model produced good simulations of the trend of the data but slightly overpredicts thyroid concentrations at later timepoints. Very good simulations of $^{36}ClO_4^-$ kinetics were achieved for all other tissues modeled.

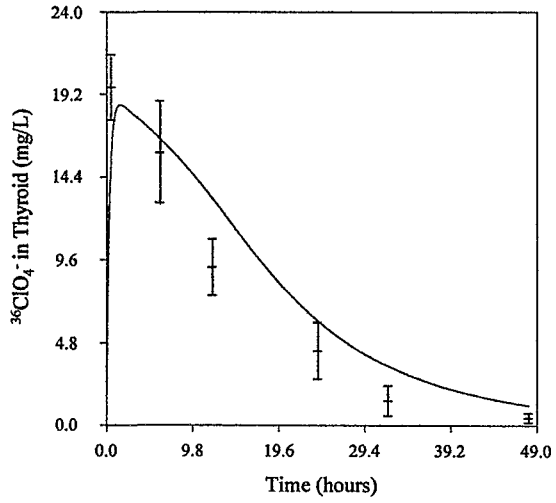

A

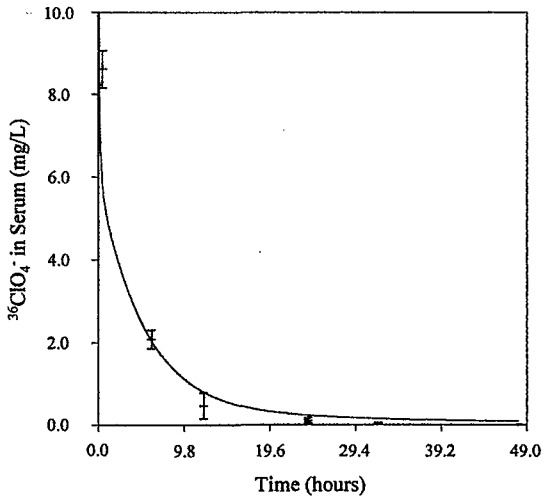

B

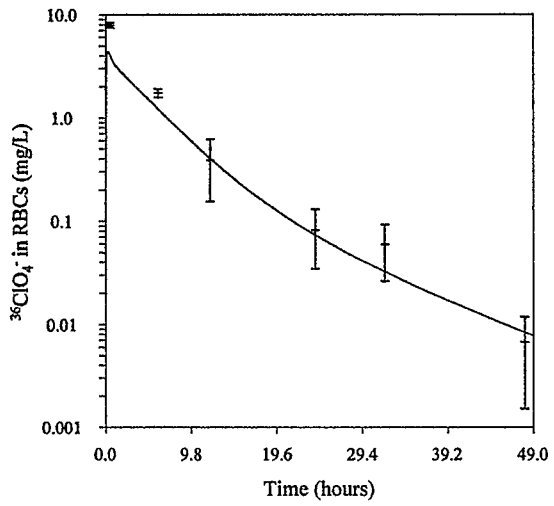
10.0
1.0
0.1
0.01
0.001
$^{36}ClO_4^-$ in RBCs (mg/L)
0.0
9.8
19.6
29.4
39.2
49.0
Time (hours)

C

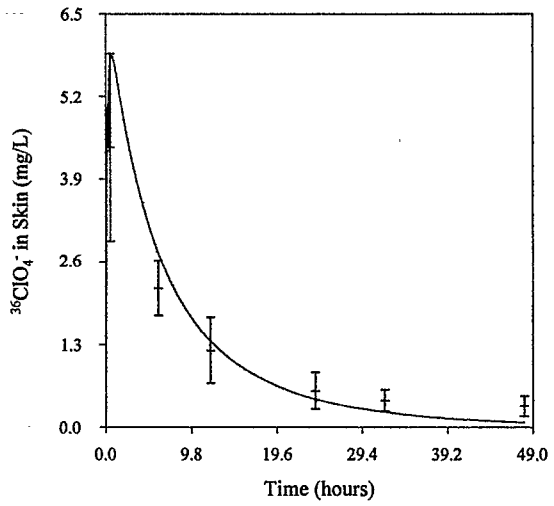
6.5
5.2
3.9
2.6
1.3
0.0
$^{36}ClO_4^-$ in Skin (mg/L)
0.0
9.8
19.6
29.4
39.2
49.0
Time (hours)

D

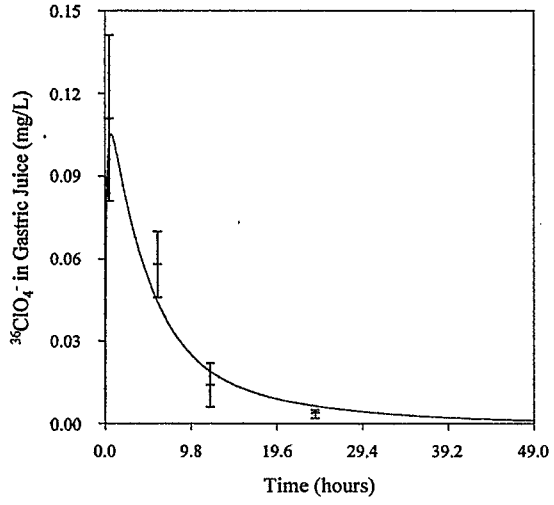
0.15
0.12
0.09
0.06
0.03
0.00
$^{36}ClO_4^-$ in Gastric Juice (mg/L)
0.0
9.8
19.6
29.4
39.2
49.0
Time (hours)

E

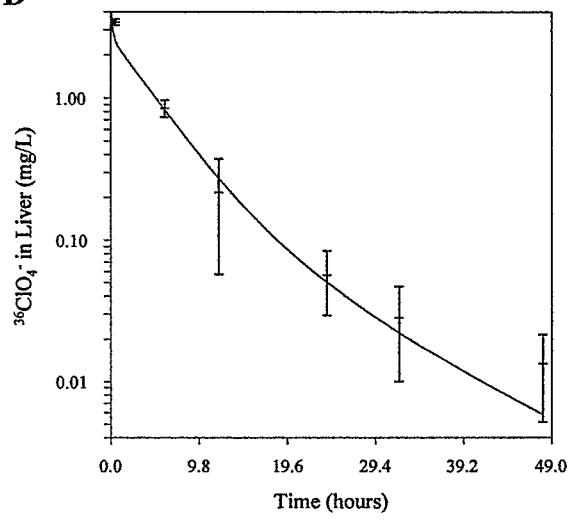
1.00
0.10
0.01
$^{36}ClO_4^-$ in Liver (mg/L)
0.0
9.8
19.6
29.4
39.2
49.0
Time (hours)

F

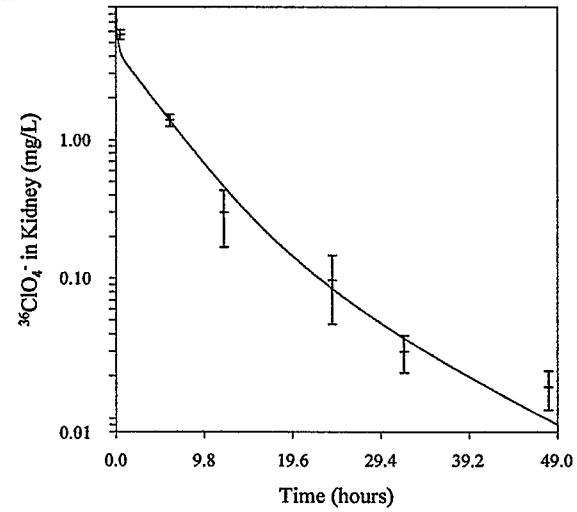
1.00
0.10
0.01
$^{36}ClO_4^-$ in Kidney (mg/L)
0.0
9.8
19.6
29.4
39.2
49.0
Time (hours)

G

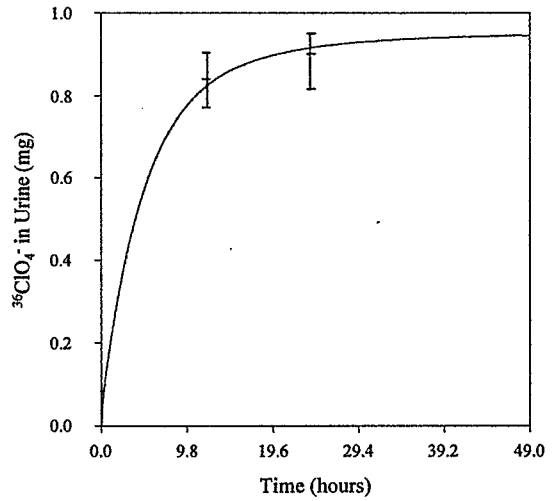
1.0
0.8
0.6
0.4
0.2
0.0
$^{36}ClO_4^-$ in Urine (mg)
0.0
9.8
19.6
29.4
39.2
49.0
Time (hours)

H

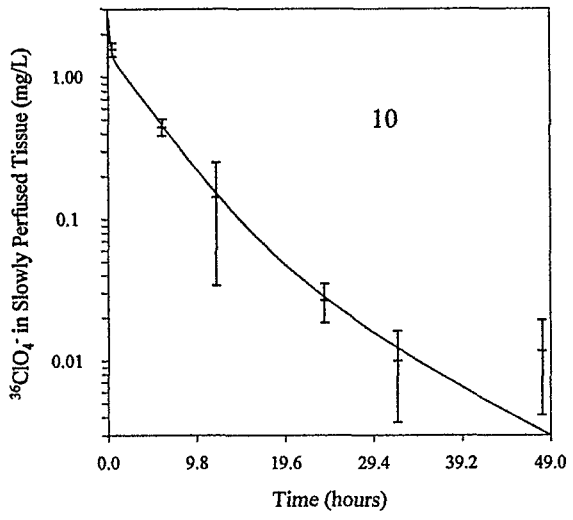

I

Figure 2. Model simulations (lines) and actual $^{36}ClO_4^-$ levels (bars) (mean ± SD) in the thyroid (A), serum (B), red blood cells (C), skin (D), gastric juice (E), liver (F), kidneys (G), urine (H) and slowly perfused tissue (I).

Thyroid, serum and urine were collected from the *iv* studies using cold perchlorate at 0.01, 0.1, 1.0 and 3.0 mg/kg. The simulations of these data sets are presented in Figures 3A and B, 4 and 5. Early model simulations at 1 mg/kg-d and below resulted in underestimation of serum perchlorate concentrations.

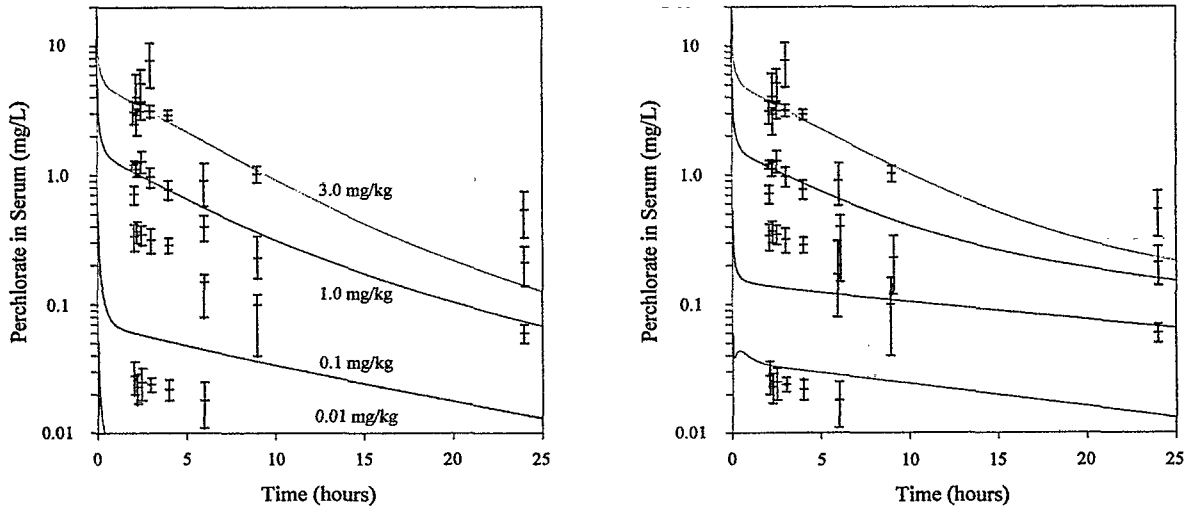

A B

Figure 3. Model predicted (lines) and actual values (dots) of perchlorate concentrations in serum with (A) and without (B) plasma binding at 3.0, 1.0, 0.1 and 0.01 mg/kg. Note that part of the simulation for the 0.01 mg/kg dose level can be seen in the lower left corner of Figure 3A.

Low serum predictions suggested either greater uptake into other tissues or protein binding. To provide better estimates of ClO_4^- serum concentrations at the 0.01 and 0.1 mg/kg doses, protein

binding code was added to the venous compartment of the model. An affinity constant (Km_Bp) of 1.1E6 ng/L and Vmaxc_Bp of 9.3E3 ng/h/kg was fitted to serum levels from doses ranging 0.01 to 3.0 mg/kg (Figure 3B). The model underpredicts serum perchlorate from the 0.1 mg/kg dose group; however it fits serum at 0.01 mg/kg and cumulative urine across the doses. Interestingly, the urinary excretion at 0.01 mg/kg was lower than the other doses, accounting for elevated serum concentrations. Mean 24 hour urinary excretions (± SD) of perchlorate were approximately 97% (± 2), 72% (± 1), 87% (± 17) and 91% (± 13) of the administered *iv* dose for the 0.01, 0.1, 1.0 and 3.0 mg/kg dose groups, respectively.

The literature discussed earlier suggests that serum albumin is the major binding protein; however it does not confirm albumin to be the only binding site. No studies were found that evaluated whether perchlorate or similar anions bind to thyroglobulin. However, Yamada (1967) studied the effects of perchlorate and other anions on T_4 metabolism and noted a significant decrease in serum protein bound iodide (PBI) in thyroidectomized T_4 maintained perchlorate-fed rats. In a 1968 *in vitro* study, Yamada and Jones reported that T_4 was displaced from plasma protein as indicated by an uptake of T_4 by muscle in the presence of plasma taken from perchlorate fed rats. He suggested that perchlorate interferes with T_4 binding with plasma proteins, but did not demonstrate it directly.

Pertechnetate is known to bind to plasma proteins. Hays and Green (1973) studied the blocking of pertechnetate binding with human serum proteins by other anions. Perchlorate was found to be one of the most effective, while iodide was ineffective. In dialysis studies, inorganic iodide did not bind to plasma proteins. The pertechnetate binding appeared to be reversible in serum.

Simulations of thyroid perchlorate concentrations from the four dose groups are shown in Figure 4. It was noted that the thyroid concentrations resulting from the 3.0 mg/kg cold perchlorate study were slightly higher than those from the $^{36}ClO_4^-$ study at 3.3 mg/kg (Figures 4 and 2A, respectively). This may reflect the analytical differences in measuring cold vs radiolabelled perchlorate. The model slightly underpredicts the thyroid concentrations at 3.0 mg/kg, based on the cold perchlorate data (Figure 4), and slightly overpredicts the $^{36}ClO_4^-$ thyroid concentration at 3.3 mg/kg.

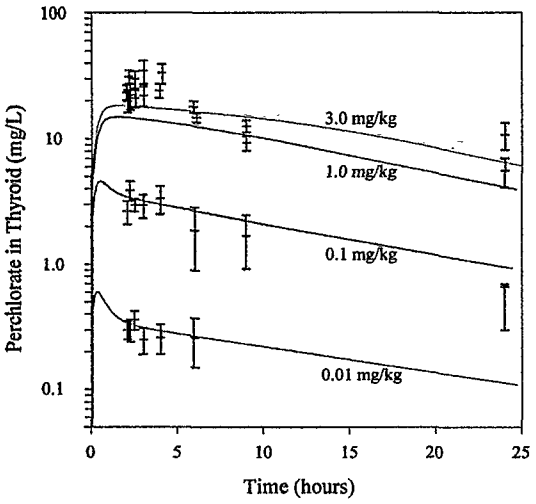

Figure 4. Model predicted (lines) and actual values (bars) of perchlorate concentration in thyroids of male rats after *iv* doses of 0.01, 0.1, 1.0 and 3.0 mg/kg.

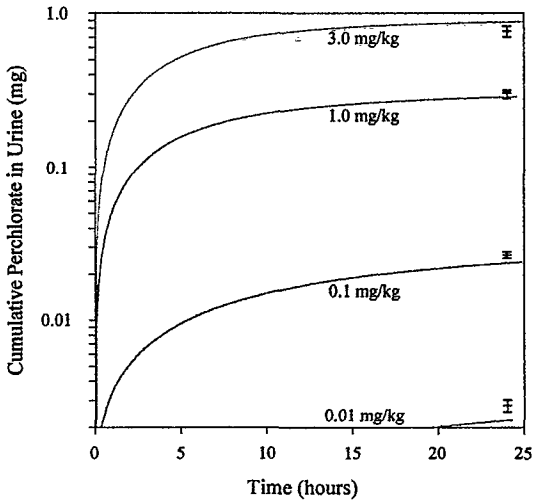

Figure 5. Model predicted (lines) and actual values (bars) of cumulative perchlorate in urine from male rats after *iv* doses of 0.01, 0.1, 1.0 and 3.0 mg/kg.

Urinary excretion of perchlorate was fitted across doses using a clearance value of 0.07 ng/h (Figure 5). This value also predicted urine perchlorate levels measured by Eichler (1929) (Figure 6).

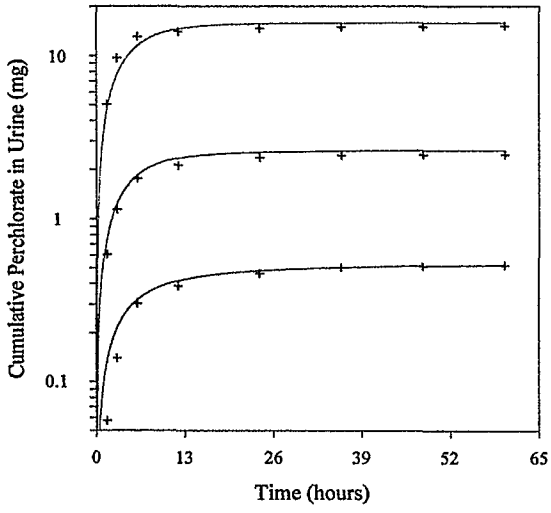

Figure 6. Cumulative ClO_4^- in urine of male rats after subcutaneous doses of 1.6, 8.0 and 49 mg/kg (Eichler, 1929)

Chow and Woodbury (1970) gave $^{36}ClO_4^-$ by *ip* administration to rats and measured radioactivity in their thyroids and serum. The rats were functionally nephrectomized by ligating the renal pedicle of both kidneys. With urinary excretion set to zero, the model adequately predicts thyroid

concentrations (Figure 7A), but underpredicts serum concentrations at 0.5 and 10.0 mg/kg (Figure 7B).

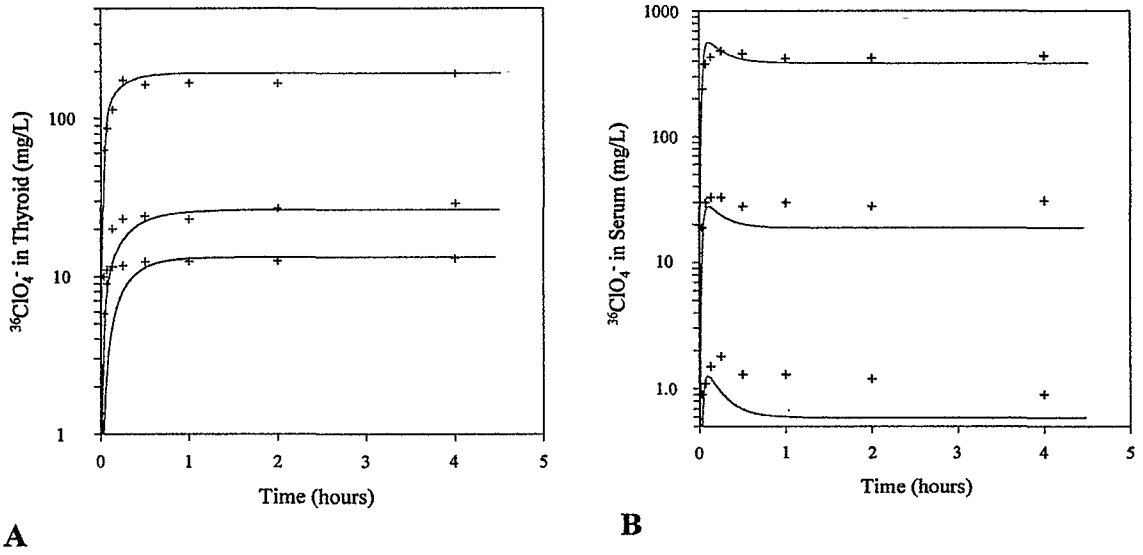

Figure 7. Model simulations (lines) and actual perchlorate concentrations in thyroid (A) and serum (B) in rats after ip administration of 0.5, 10.0 and 200 mg/kg $^{36}ClO_4^-$ (Chow and Woodbury, 1970).

The underprediction of serum would suggest increased plasma binding is required. However, that is not consistent with our findings, since the model adequately simulates our results at lower dose levels. Analytical differences between Chow and Woodbury's results and ours are a possibility. It is also possible that blocking kidney discharge creates physiological effects that the model does not sufficiently account for by simply turning off urinary excretion. One hypothesis is that saturation in NIS containing tissues occurs to a lesser extent as a result of increased extracellular Na^+ and possibly competitive anions when renal clearance is blocked. Thereby, the arterial $^{36}ClO_4^-$ concentration could increase to a greater extent than the model's physiology predicts.

Parameterization of the Iodide Model

Model predictions of acute $^{125}I^-$ (with carrier) kinetics in the thyroid, serum, stomach contents, skin and urine are presented in Figures 8 through 10. These figures represent an *iv* dose of 0.033 mg/kg $^{125}I^-$ with carrier.

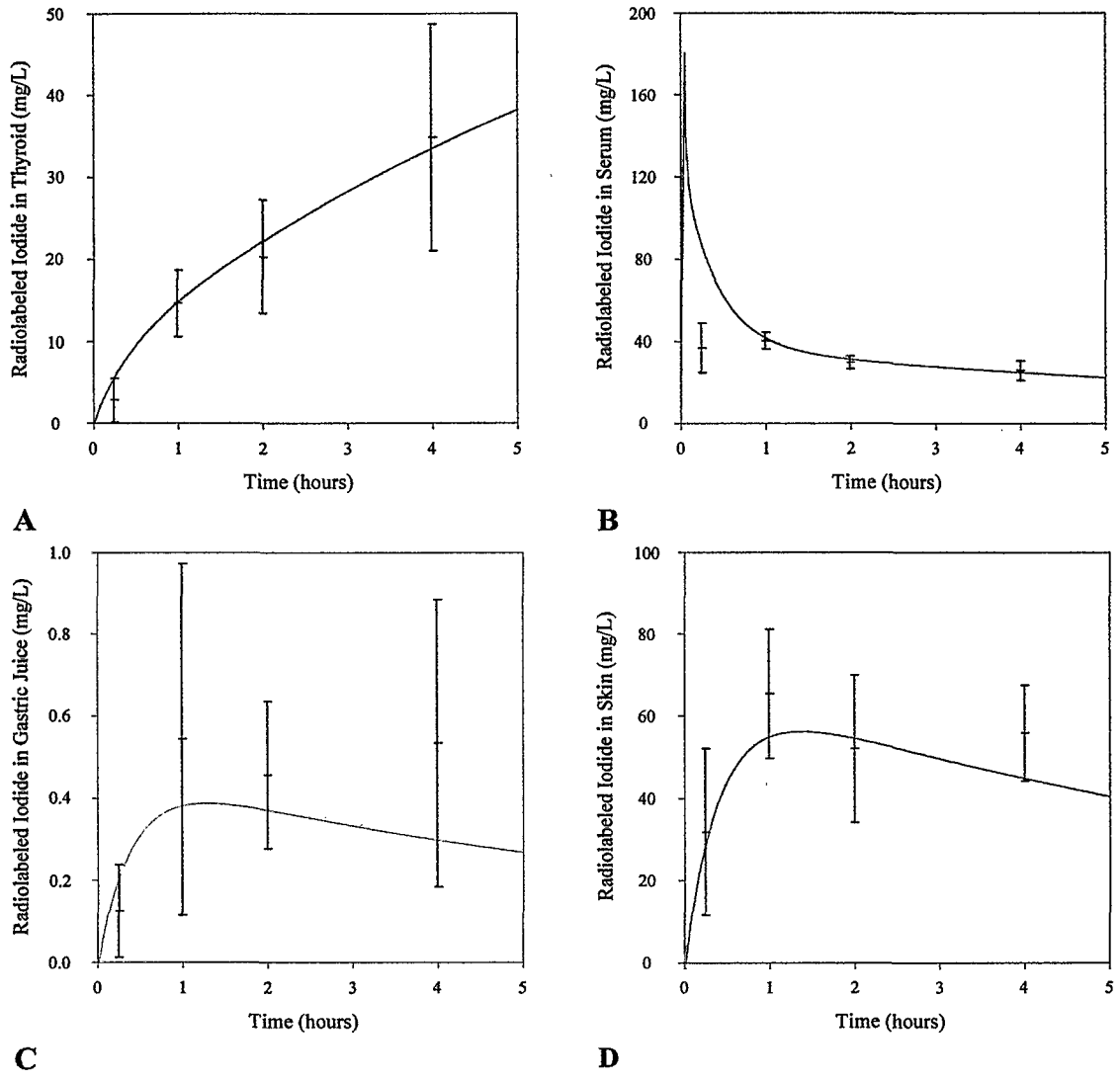

Figure 8. Model predicted (lines) and actual values (mean ± SD) of $^{125}I^-$ in thyroid (A), serum (B), stomach contents (C) and skin (D) of male rats after an *iv* dose of 0.033 mg/kg $^{125}I^-$ with carrier.

Interestingly, the simulated amount of $^{125}I^-$ in stomach contents indicates that although there is very rapid uptake of iodide and perchlorate into gastric juice, it is quickly reabsorbed in the gut lumen. GI clearance of iodide is rapid and plays an important role in radioiodide conservation. The skin also exhibits a rapid uptake of both iodide (Figure 8D) and perchlorate (Figure 2D) but clearance is slow.

Figures 9A through C show model simulations from a second study where urine was collected. The amount of iodide in the thyroid simulations represents total iodine, including iodinated hormones and precursors. Figure 10A demonstrates that the model predicts well the amount in the thyroid over 96 hours after dosing.

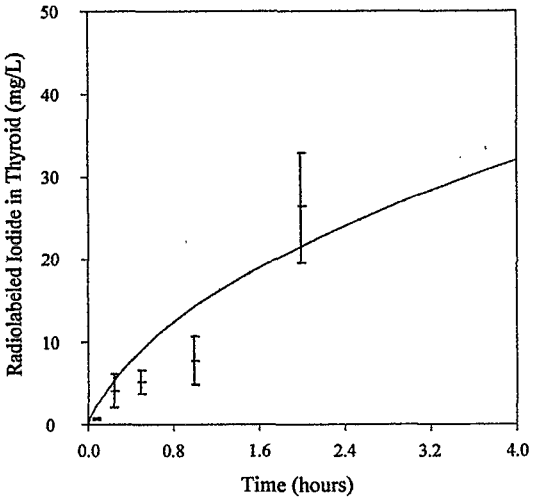

A

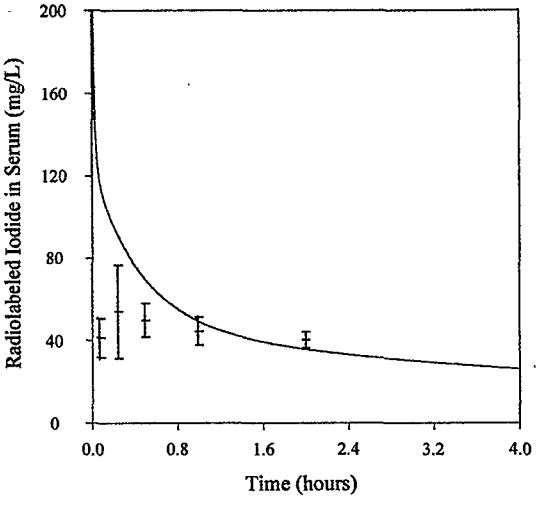

B

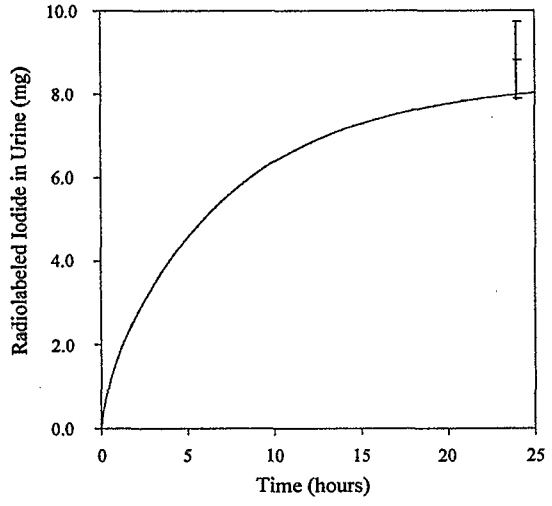

C

Figure 9. Radiolabeled iodide in thyroid (A), serum (B) and urine (C) from male rats after an *iv* dose of 0.033 mg/kg $^{125}I^-$ with carrier. Model predicted (lines) and actual values (mean ± SD) shown.

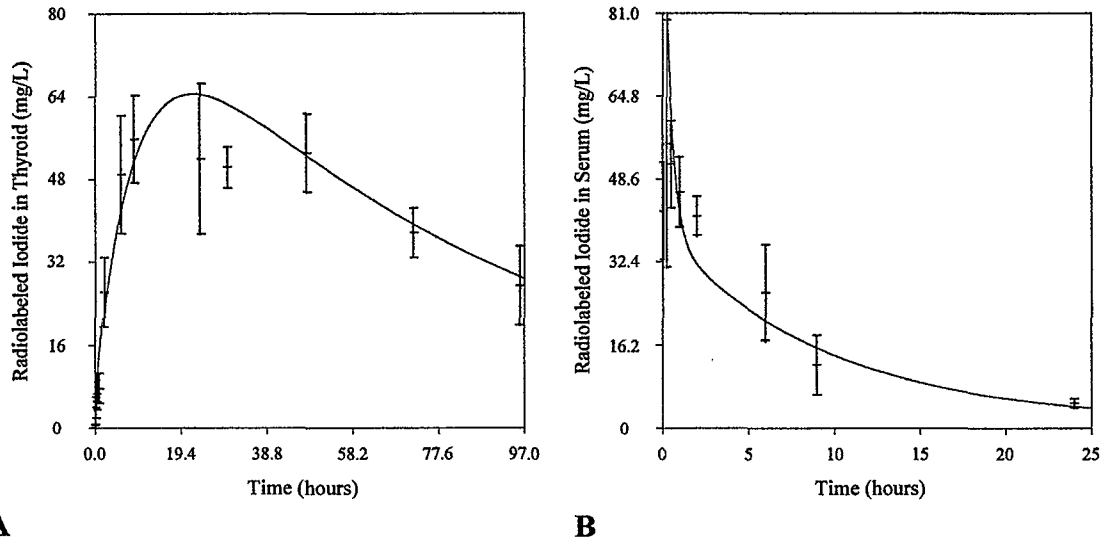

Figure 10. Iodide in thyroid (A) and serum (B) from male rats following *iv* administration of 0.33 mg/kg $^{125}I^-$ with carrier. Model predicted (lines) and actual values (mean ± SD) shown.

Inhibition of Thyroid Iodide Uptake After Acute Dose of Perchlorate

Inhibition of $^{125}I^-$ uptake into the thyroid following *iv* doses of 0, 0.01, 0.1, 1.0 and 3.0 mg/kg perchlorate was simulated using the parameters listed in Tables 1 and 2 (Figure 11). Perchlorate-induced inhibition of $^{125}I^-$ uptake in the thyroid was 13, 24, 70 and 88% at 2 hours and 11, 29, 55 and 82% at 9 hours after dosing with $^{125}I^-$ with carrier for the 0.01, 0.1, 1.0 and 3.0 mg/kg dose groups. Good simulations were achieved across doses. However, at 3.0 mg/kg, the model slightly overpredicts inhibition 6 hrs after the perchlorate dose (4 hours after $^{125}I^-$ administration). TSH was measured from the highest dose level (3.0 mg/kg) between 8 and 48 hours post dosing and was found to increase between 8 and 12 hrs. It is possible that TSH was already elevated at 6 hrs, allowing upregulation of the thyroid to compensate for inhibition at that time point, which the model would not predict. Yu *et al.* (2000a) provides greater details on hormone fluctuations resulting from our studies.

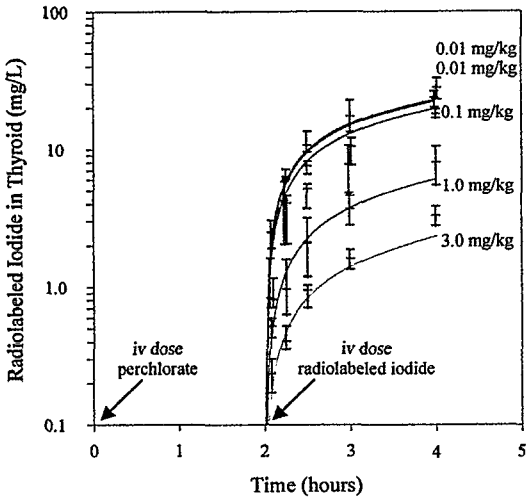

Figure 11. Iodide uptake inhibition in male rats intravenously administered ClO_4^-, followed by 33 μg/kg $^{125}I^-$ with carrier two hours later. Model simulations (smooth lines) and actual data ± SD (vertical lines) for $^{125}I^-$ in thyroid after 0, 0.01, 0.1, 1.0 and 3.0 mg/kg ClO_4^- (inhibition from 0.0 and 0.01 mg/kg ClO_4^-) overlap.

Perchlorate Drinking Water Kinetics

Figures 12 and 13 show the serum and thyroid perchlorate concentrations at 0.01, 0.1, 1.0, 3.0, 10.0 and 30.0 mg/kg-d. The model was programmed to simulate oral dosing for 12 hours per day, assuming rats drink fairly continuously during their waking hours. The same perchlorate parameters used to described acute kinetics adequately described serum concentrations from chronic exposure (Figure 12), but failed to predict thyroid concentrations from the higher doses (e.g., 3.0 mg/kg-d and higher) (Figure 13A). TSH levels increased during drinking water exposures across all doses (data not shown). To account for TSH induced up-regulation, the thyroid concentrations from the 3.0, 10.0 and 30.0 mg/kg-d dose groups were fitted by increasing the effective follicle:stroma partition coefficient (PT_p) (Figure 13B).

TSH is not expected to increase NIS in tissues other than the thyroid (Brown-Grant, 1961). Our results agree. Given the small size of the thyroid, its up-regulation would not decrease serum concentrations significantly. This explains why the model successfully predicted serum perchlorate concentrations across drinking water doses with the same parameters used to describe acute exposures, but could not predict thyroid concentrations above 3 mg/kg-d.

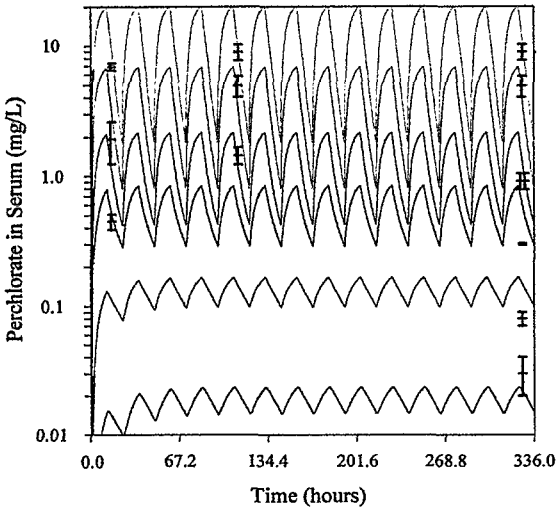

Figure 12. Serum perchlorate concentrations in male rats ingesting 0.01, 0.1, 1.0, 3.0, 10 and 30 mg/kg-d perchlorate in drinking water for 14 days. Model predicted (lines) and actual values (Mean ± SD) presented.

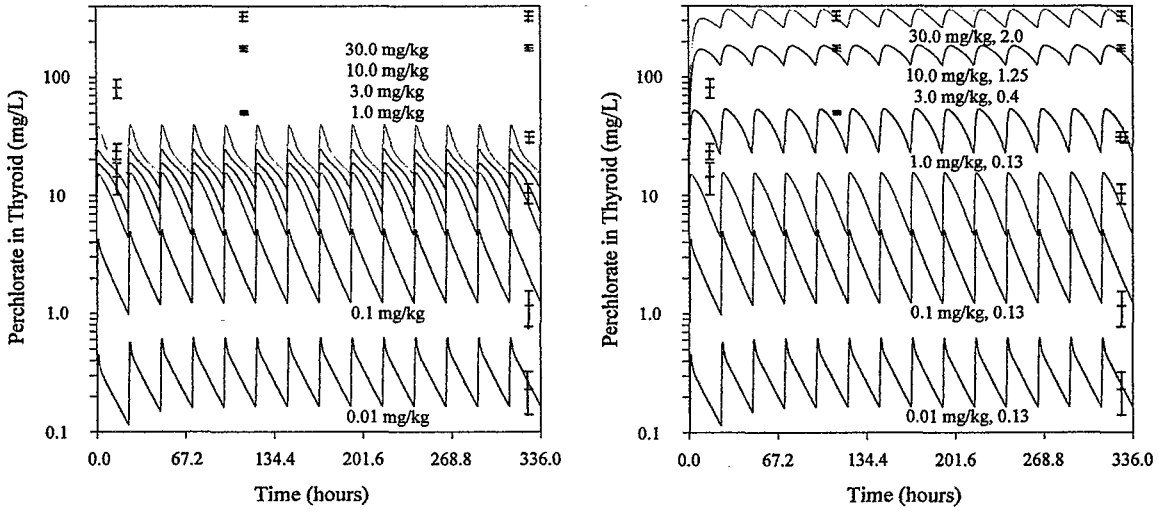

Figure 13. Model prediction (lines) and actual data means ± SD (bars) of thyroid perchlorate concentrations in male rats during ingestion of 0.01, 0.1, 1.0, 3.0, 10 and 30 mg/kg-d perchlorate in drinking water for 14 days. Simulations using thyroid parameters established from acute dosing (A) fail to predict concentrations at 3.0, 10 and 30 mg/kg-d. Data across doses (B) can be fit by increasing the follicle:stroma effective partitioning (PT_p) from 0.13 to 0.4 at 3 mg/kg-d, 1.25 at 10 mg/kg-d and 2.0 at 30 mg/kg-d.

Inhibition of Thyroid ^{125}I Uptake After Exposure to Perchlorate in Drinking Water

Figure 14 shows inhibition of iodide uptake into the thyroid after 14 days of drinking water exposure to perchlorate at 0.01, 0.1, 1.0, 3.0, 10.0 and 30.0 mg/kg-d. The model overpredicts inhibition at 1.0 mg/kg-d and greater. TSH-induced up-regulation of the thyroid compensates for competitive inhibition, resulting in little or no inhibition of radioiodide uptake on day 14 of exposure in all dose groups except 30 mg/kg-d.

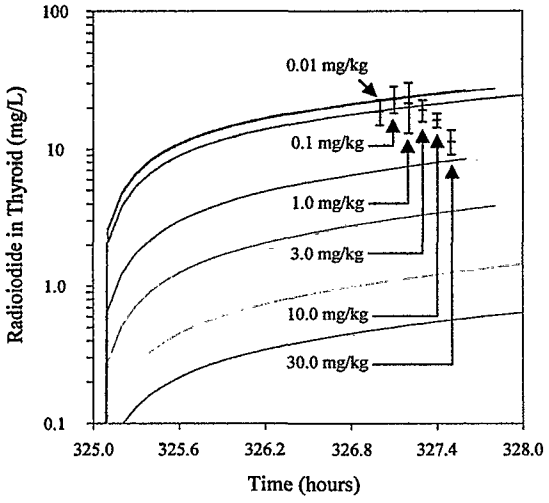

Figure 14. Iodide uptake inhibition in male rats after administration of ClO_4^- in drinking water for 14 days, followed by an *iv* dose of 33 μg/kg $^{125}I^-$ with carrier. Model simulations (smooth lines) and actual data ± SD (vertical lines) are shown for $^{125}I^-$ in thyroid after 0, 0.01, 0.1, 1.0, 3.0, 10.0 and 30.0 mg/kg-d ClO_4^-.

In all treated groups, TSH levels were already increased after the first day. Serum T_4 initially decreased in all dose groups except the 0.01 mg/kg-d group. By day 14, T_4 levels had increased to control values in the 0.1 and 1.0 mg/kg-d dose groups. FT_4 increased in all dose groups on day 1, returned to normal values by day 5 and were significantly elevated across all dose groups by day 14, except the 0.1 mg/kg-d group. Details on the hormone results from this study are provided in Yu *et al.* (2000a).

CONCLUSION

The proposed PBPK model for ClO_4^- and I^- kinetics has been used to predict internal dose of ClO_4^- and thyroid I^- inhibition. Simulations have shown good correspondence between predicted tissue compartment concentrations and measured values in the thyroid, serum, red blood cells, urine, liver, muscle, skin and stomach in the rat. The model structure of the thyroid requires three compartments (stroma, follicle and colloid) to quantify rapid organification in the gland.

Differences in model parameters between iodide and perchlorate indicate that iodide kinetics are very similar to perchlorate kinetics, but cannot be applied directly. The main differences involve the saturable kinetics of the thyroid, skin and stomach, with perchlorate exhibiting higher

the saturable kinetics of the thyroid, skin and stomach, with perchlorate exhibiting higher Vmax's except in the skin. Because organification of iodide occurs in both the thyroid follicle and colloid, their respective Vmax's are over 1000 and 10 times higher than those for perchlorate, which is discharged unchanged. Perchlorate affinity for the symporters into the follicle and colloid were approximately an order of magnitude greater (lower Km) than those of iodide.

The thyroid perchlorate concentrations from high drinking water exposures were fitted by increasing the effective follicle:stroma partition coefficient (PT_p) to account for TSH stimulation. However, it is expected that other parameters (e.g., follicle size and follicular Vmax) would also increase. In fact, TSH stimulation results in several changes in the thyroid. There is an increase in percent of thyroid volume attributed to the follicle cells (Conde *et al.*, 1991; Ginda *et al.*, 2000), total protein, RNA and DNA content, and the incorporation of labeled aminoacids into protein (Pisarev and Kleiman de Pisarev, 1980). Predictions could be achieved by adjusting additional parameters, but without incorporation of the hypothalamic-pituitary-thyroid axis, such adjustments provide little additional insight at this point.

The model, however, could simulate serum concentrations from drinking water exposures using parameters established from the acute data. The thyroid, given it's small size, would not be expected to significantly alter serum concentrations, even during hyperstimulation. Although TSH has not been shown to increase the NIS in other tissues, NIS-containing tissues were not obtained from our drinking water study to support this.

Urinary clearance values of 0.05 L/h for iodide and 0.07 L/h for perchlorate were used across data sets. The model supports plasma binding; a saturable term is required to simulate serum concentrations at lower doses. It is possible that perchlorate competes with thyroxine for the same binding sites of plasma proteins, as the work of Yamada and Jones (1968) suggests.

While there are limited data suggesting iodide and perchlorate uptake in the skin, the model and the kinetic studies support this assumption. Without the skin compartment, the model overestimated circulating plasma inorganic iodide and perchlorate. Due to its large size, skin appears to be an important pool for slow turnover of these anions. Brown-Grant (1961) noted that the uptake of iodide was higher in the male rat and pup than in the female. Our findings agree, with the model requiring a higher Vmax in the skin for the male rat than that reported for the pregnant rat (Clewell *et al.*, 2001a).

Further definition and refinement of the model is expected from efforts to identify thyroid hormone and histological changes produced by perchlorate exposure. This will require expansion of the model to a true endogenous iodide model, including subsequent thyroid hormone synthesis and regulation. Dietary iodide and endogenous inorganic iodide levels will clearly be required because excessive iodide intake can inhibit its own uptake. Plasma inorganic iodide is rarely reported in the literature due to the difficult nature of its analysis. While measurements of tracer radioiodide can be fitted to predict transfer rates, its use is limited when attempting to predict the saturation of nonlinear compartments, such as the thyroid, which are dependent upon existing amounts of iodide already present. Subsequent modeling efforts on

predicting thyroid hormone production will require plasma inorganic iodide, in addition to thyroid hormone levels.

The present PBPK model for ClO_4^- and I^- will be useful to improve the dose-response evaluation of adverse effects after ClO_4^- exposure. In addition, the model is expected to improve the accuracy of interspecies extrapolation in the 2001 revised US EPA assessment of perchlorate. The relevance to chronic exposure at low levels in pregnant humans, a population of concern, is not fully established at this point. However, pregnant and lactating rat models have been developed by Clewell *et al.* (2001a, 2001b), which accurately predict the dose to the fetal rat and to the neonate through nursing. In conjunction with our human model (Merrill *et al.*, 2001), potential future development of all these models could include extrapolation to pregnant and lactating humans.

ACKNOWLEDGEMENTS

The animals used in in-house studies were handled in accordance with the principles stated in the *Guide for the Care and Use of Laboratory Animals*, National Research Council, 1996, and the Animal Welfare Act of 1966, as amended.

We thank Lt Col Dan Rogers and Dr. David Mattie, U.S. Air Force, for assistance in obtaining funding of this research and for funding from NASA and the US Navy. Lastly, this work would not have been possible without the critical laboratory support of Latha Narayanan, Eric Eldridge, Dick Godfrey, Paula Todd, Tim Bausman and Susan Young. In addition, gratitude is extended to Mel Andersen for providing modeling input.

REFERENCES

Ajjan, R.A., Kamaruddin, N.A., Crisp, M., Watson, P.F., Ludgate, M., and Weetman, A.P. 1998. Regulation and tissue distribution of the human sodium iodide symporter gene. Clin.Endocrinol. 49: 517-523.

Altman, P.L. and D.S. Dittmer. 1971a. Volume of blood in tissue: Vertebrates. In: *Respiration and Circulation.* Bethesda, MD: Federation of American Societies for Experimental Biology. p. 383-387.

Altman, P.L. and D.S. Dittmer. 1971b. Blood volumes. In: *Respiration and Circulation.* Bethesda, MD: Federation of American Societies for Experimental Biology. p. 376-383.

Anbar, M., S. Guttmann, and Z. Lewitus. 1959. The mode of action of perchlorate ions on the iodine uptake of the thyroid gland. Int.J.Appl.Radiat.Isot. 7: 87-96.

Bagchi, N. and Fawcett, D.M. 1973. Role of sodium ion in active transport of iodide by cultured thyroid cells. Biochim.Biophys.Acta 318: 235-251.

Bernal, J. and Nunez, J. 1995. Thyroid hormones and brain development. Eur.J.Endocrinol. 133: 390-398.

Brown-Grant, K. and G. Pethes. 1959. Concentration of radio-iodide in the skin of the rat. J.Physiol. 148: 683-693.
Brown-Grant, K. 1961. Extrathyroidal iodide concentrating mechanisms. Physiolog.Rev. 41: 189-213.

Brown, R.P., M.D. Delp, S.L. Lindstedt, L.R. Rhomberg, and R.P. Beliles. 1997. Physiological parameter values for physiologically based pharmacokinetic models. Toxicol.Ind.Health 13: 407-484.

Carr, C.W. 1952. Studies on the binding of small ions in protein solutions with the use of membrane electrodes. I. The binding of the chloride ion and other inorganic anions in solutions of serum albumin. Arch.Biochem.Biophys. 40: 286-294.

Chow, S.Y., Chang, L.R., and Yen, M.S. 1969. A comparison between the uptakes of radioactive perchlorate and iodide by rat and guinea-pig thyroid glands. J.Endocrinol. 45: 1-8.

Chow, S.Y. and Woodbury, D.M. 1970. Kinetics of distribution of radioactive perchlorate in rat and guinea-pig thyroid glands. J.Endocrinol. 47: 207-218.

Clewell, R.A., Merrill, E.M., Yu, K.O., Mahle, D.A., Sterner, T.R., Robinson, P.J., and Gearhart, J.M. 2001a. Physiologically-based pharmacokinetic model for the kinetics of perchlorate-induced inhibition of iodide in the pregnant rat and fetus. AFRL-HE-WP-CL-2001-0006.

Clewell, R.A., Merrill, E.M., Fisher, J.W., Yu, K.O., Mahle, D.A., Sterner, T.R., and Gearhart, J.M. 2001b. Physiologically-based pharmacokinetic model for the kinetics of perchlorate-induced inhbition of iodide in the lactating and neonatal rat. AFRL-HE-WP-CL-2001-0007.

Conde, E., Martin, L., I, Gonzalez, C.R., and Galera, D.H. 1991. Histometry of normal thyroid glands in neonatal and adult rats. Am.J.Anat. 191: 384-390.

Durand, J. 1938. Recherches sur l'elimination des perchlorates, sur leur repartition dans les organes et sur leur toxicite. [Research on the elimination of perchlorate, its distribution in organs and its toxicity]. Bull.Soc.Chim.Biol. 20: 423-433.

Eichler, O. 1929. Zur Pharmakologie der Perchloratwirkung [The pharmacology of the perchlorate effect]. Naunyn-Schmiedeberg's Arch.Exp.Path.u.Pharmak 144: 251-260.

Fisher, J.W, Narayanan, L, Godfrey, R.J., Todd, P.N., Bausman, T.A., Young, S.M., Sterner, T.R., Mattie, D.R., and Yu, K.O. 2000. Physiological model for inhibition of thyroidal uptake of iodide by perchlorate in the rat. AFRL-HE-WP-CL-2000-0035.

Ginda, W.J., Nowak, K.W., and Malendowicz, L.K. 2000. Decrease of TSH levels and epithelium/colloid ratio in rat thyroid glands following administration of proadrenomedullin N-terminal peptide (12-20). Horm.Metab.Res. 32: 10-14.

Gluzman, B.E. and H. Niepomniszcze 1983. Kinetics of the iodide trapping mechanism in normal and pathological human thyroid slices. Acta.Endocrinol.Copenh. 103: 34-39.

Golstein, P., Abramow, M., Dumont, J.E., and Beauwens, R. 1992. The iodide channel of the thyroid: a plasma membrane vesicle study. Am.J.Physiol. 263: C590-7.

Halmi, N.S., Stuelke, R.G. and Schnell M.D. 1956. Radioiodide in the thyroid and in other organs of rats treated with large doses of perchlorate. Endocrinology 58: 634-650.

Halmi, N.S. and Stuelke, R.G. 1959. Comparison of Thyroidal and Gastric Iodide Pumps in Rats. Endocrinology 64: 103-109.

Hanwell, A. and Linzell, J.L. 1973. The time course of cardiovascular changes in lactation in the rat. J Physiol.Lond. 233: 93-109.

Harden, R.M., Alexander, W.D., Shimmins, J., and Chisholm, D. 1968. A comparison between the gastric and salivary concentration of iodide, pertechnetate, and bromide in man. Gut 10: 928-930.

Hays, M.T. and Green, F.A. 1973. *In vitro* studies of 99m Tc-pertechnetate binding by human serum and tissues. J.Nucl.Med. 14: 149-158.

Hetzel, B.S. 1983. Iodine deficiency disorders (IDD) and their eradication. Lancet 2: 1126-1129.

Honour, A.J., N.B. Myant, and E.N. Rowlands. 1952. Secretion of radioiodine in digestive juices and milk in man. Clin.Sci. 11: 447-463.

Kotani, T., Ogata, Y., Yamamoto, I., Aratake, Y., Kawano, J.I., Suganuma, T., and Ohtaki, S. 1998. Characterization of gastric Na^+/I^- symporter of the rat: Clin.Immunol.Immunopathol. 89: 271-278.

Kotyk, A. and K. Janacek. 1977. *Membrane Transport. An Interdisciplinary Approach.* New York: Plenum Press.

Lazarus, J.H., Harden, R.M., and Robertson, J.W. 1974. Quantitative studies of the inhibitory effect of perchlorate on the concentration of 36ClO minus 4, 125I minus and 99mTcO minus 4 in salivary glands of male and female mice. Arch.Oral Biol. 19: 493-498.

Malendowicz, L.K. 1977. Sex dimorphism in the thyroid gland. I. Morphometric studies on the thyroid gland of intact adult male and female rats. Endokrinologie. 69: 326-328.

Malik, A.B., Kaplan, J.E., and Saba, T.M. 1976. Reference sample method for cardiac output and regional blood flow determinations in the rat. J Appl.Physiol. 40: 472-475.

Merrill, E.A., Clewell, R.A., Sterner, T.R., Gearhart, J.M. 2001. PBPK model for perchlorate-induced inhibition of radioiodide uptake in humans. AFRL-HE-WP-CL-2001-0008.

Pena, H.G., Kessler, W.V., Christian, J.E., Cline, T.R., and Plumlee, M.P. 1976. A comparative study of iodine and potassium perchlorate metabolism in the laying hen. 2. Uptake, distribution, and excretion of potassium perchlorate. Poult.Sci. 55: 188-201.

Perlman, I., Chaikoff, I.L., and Morton, M.E. 1941. Radioactive iodine as an indicator of the metabolism of iodine. I. The turnover of iodine in the tissues of the normal animal, with particular reference to the thyroid: J.Biol.Chem. 139: 433-447.

Pisarev, M.A. and Kleiman de Pisarev, D.L. 1980. Biochemistry of thyroid regulation under normal and abnormal conditions. J.Endocrinol.Invest. 3: 317-329.

Rall, J.E., Power, M.H., and Albert, A. 1950. Distribution of radioiodine in erythrocytes and plasma of man. Proc.Soc.Exp.Biol.Med. 74: 460-461.

Ribela, M.T.C.P., Marone, M.M.S., and Bartolini, P. 1999. Use of radioisotope urinalysis for effective thyroid blocking in the first few hours post exposure. Health.Phys. 76: 11-16.

Scatchard, G. and Black, E.S. 1949. The effect of salts on the isoionic and isoelectric points of proteins. J.Phys.Colloid Chem. 53: 88-99.

Shishiba, Y., Shimizu, T., Yoshimura, S., and Shimizu, K. 1970. [Effect of thiocyanate and perchlorate on free thyroxine fraction]. Nippon.Naibunpi.Gakkai.Zasshi. 46: 16-19.

Spitzweg, C., Joba, W., Eisenmenger, W., and Heufelder, A.E. 1998. Analysis of human sodium iodide symporter gene expression in extrathyroidal tissues and cloning of its complementary deoxyribonucleic acids from salivary gland, mammary gland, and gastric mucosa. J.Clin.Endocrinol.Metab. 83: 1746-1751.

Spitzweg, C., Heufelder, A.E., and Morris, J.C. 2000. Thyroid iodine transport. Thyroid 10: 321-330.

Urbansky, E.T. and Schock, M.R. 1999. Issues in managing the risks associated with perchlorate in drinking water. J.Environ.Management. 56: 79-95.

Wolff, J. and Maurey, J.R. 1961. Thyroidal iodide transport: II. Comparison with non-thyroid iodide-concentrating tissues: Biochim.Biophys.Acta 47: 467-474.

Wolff J. and Maurey, J.R. 1963. Thyroidal iodide transport. IV. The role of ion size. Biochim.Biophys.Acta. 69: 48-58.

Wolff, J. 1998. Perchlorate and the thyroid gland. Pharmacolog.Rev. 50: 89-105.

Wyngaarden, J.B., Wright, B.M., and Ways, P. 1952. The effect of certain anions upon the accumulation and retention of iodide by the thyroid gland. Endocrinology 50: 537-549.

Yamada, T. and Jones, A. 1968. Effect of thiocyanate, perchlorate and other anions on plasma protein-thyroid hormone interaction *in vitro*. Endocrinology 82: 47-53.

Yamada, T. 1967. Effects of perchlorate and other anions on thyroxine metabolism in the rat. Endocrinology 81: 1285-1290.

Yu, K.O., Todd, P.N., Bausman, T.A., Young, S.M., Mattie, D.R., Fisher, J.W., Narayanan, L., Godfrey, R.J., Goodyear, C.D. and Sterner, T.R. 2000a. Effects of perchlorate on thyroidal uptake of iodide with corresponding hormonal changes. AFRL-HE-WP-TR-2000-0076.

Yu, K.O., Mahle, D.A., Narayanan, L., Godfrey, R.J., Buttler, G.W., Todd, P.N., Parish, M.A., McCafferty, J.D., Ligman, T.A., Goodyear, C.D., Sterner, T.R., Bausman, T.A., Mattie, D.R. and Fisher, J.W. 2000b. Tissue distribution and inhibition of iodide uptake in the thyroid by perchlorate with corresponding hormonal changes in pregnant and lactating rats (drinking water study). AFRL-HE-WP-CL-2000-0038.

Zeghal, N., M. Redjem, F. Gondran, and E. Vigouroux. 1995. Analysis of iodine compounds in young rat skin in the period of suckling and in the adult. Effect of perchlorate. Arch.Physiol.Biochem. 103: 502-511.